

Coordination Polymerization of Metal Azides and Powerful Nitrogen-Rich Ligand toward Primary Explosives with Excellent Energetic Performances

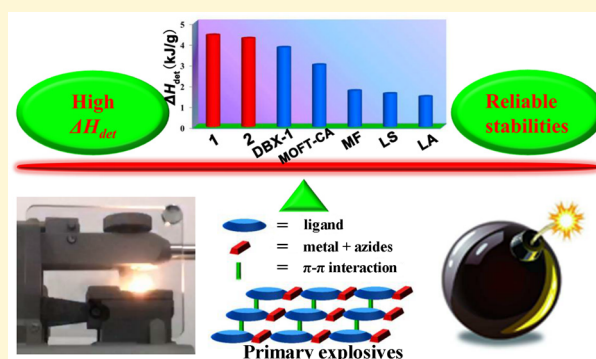
Jian-Gang Xu,^{†,‡} Cai Sun,^{†,‡} Ming-Jian Zhang,[†] Bin-Wen Liu,^{†,‡} Xiao-Zhen Li,^{†,‡} Jian Lu,^{†,‡} Shuai-Hua Wang,[†] Fa-Kun Zheng,^{*,†,‡} and Guo-Cong Guo^{*,†,‡}

[†]State Key Laboratory of Structural Chemistry, Fujian Institute of Research on the Structure of Matter, Chinese Academy of Sciences, Fuzhou, Fujian 350002, P. R. China

[‡]University of Chinese Academy of Sciences, Beijing 100039, P. R. China

Supporting Information

ABSTRACT: Advancement in explosive systems toward miniaturization and enhanced safety has prompted the development of primary explosives with powerful detonation performance and relatively low sensitivities. Energetic coordination polymers (ECPs) as a new type of energetic materials have attracted wide attention. However, regulating the energetic characters of ECPs and establishing the relationship between structure and energetic property remains great challenges. In this study, two isomorphous 2D π -stacked solvent-free coordination polymers, $[M(N_3)_2(atrz)]_n$ ($M = Co$ 1, Cd 2; $atrz = 4,4'$ -azo-1,2,4-triazole), were hydrothermally prepared and structurally characterized by X-ray diffraction. The two compounds exhibit reliable stabilities, remarkable positive enthalpies of formation, and prominent heats of detonation. The enthalpy of formation of 1 is $4.21 \text{ kJ}\cdot\text{g}^{-1}$, which is higher than those of all hitherto known primary explosives. Repulsive steric clashes between the sensitive azide ions in 1 and 2 influence the mechanical sensitivities deduced from the calculated noncovalent interaction domains. The two energetic π -stacked ECPs 1 and 2 can serve as candidates for primary explosives with an approved level of safety.



INTRODUCTION

Primary explosives, as the most widely used energetic materials, are essential in explosive systems. These initiators rapidly shift deflagration to detonation to produce a powerful blast wave that initiates a stronger secondary explosive.¹ Lead styphnate (LS), lead azide (LA), and mercury fulminate (MF) have long been used as the most commonly used primary explosives.^{2,3} However, because explosive compounds are being developed toward miniaturization and enhanced safety direction, energetic performances of the system of LS and LA primary explosives hardly satisfy the demands.^{4,5} Therefore, a new class of primary explosives that will replace lead/mercury-based primary explosives should possess the following properties: (a) powerful energetic performance; (b) simple and safe synthesis; (c) stability to at least 180°C and insensitivity to light; (d) relative low mechanical and electrostatic discharge sensitivity (ESD) (avoid being insensitive to ignition) for handling, storage, and transport; (e) solvent-free; and (f) few toxic metals and perchlorate-free.⁶

Many studies have focused on the exploration of new primary explosives to meet aforementioned requirements. These explorations can be classified into two methods. Numerous transition-metal azides such as copper azide (CA),

cobalt azide, and cadmium azide possess high power blasting power.⁷ Nevertheless, high sensitivities, danger during preparation, complex synthesis, and low thermal decomposition temperature limit the practical applications of these azides as primary explosives.⁷ Modifying existing transition-metal azides by utilizing insensitive materials to reduce the sensitivities of these azides is one approach to overcome these limitations. For example, in 2010, Gogotsi's group reported CA confined inside templated carbon nanotubes to improve electrical conductivity to reduce ESD (Scheme S1a).⁸ In 2016, Wang and his coworkers creatively used carbonized metal–organic frameworks (MOFs) as the conductive porous carbon matrix template synthesis of CA (MOFT-CA) as the primary explosive with relatively low sensitivities (Scheme S1b).⁹ Yet, the heat of detonation (ΔH_{det}) could inevitably decrease with the introduction of carbon materials. Synthesizing new powerful compounds such as potassium dinitraminobistetrazolate (K_2 DNABT),⁶ potassium 4,5-bis(dinitromethyl)furoxanate (KDNMFO),¹⁰ and 4,4'-bis(dinitromethyl)-3,3'-azofurazanate

Received: August 15, 2017

Revised: October 24, 2017

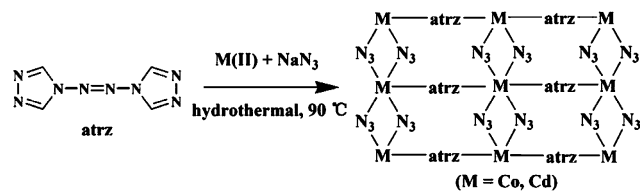
Published: November 3, 2017

(KDNMAFZ),¹¹ is another solution. However, this approach frequently involves complex and risky synthesis.^{6,10,11} Despite these advancements, high energy, desired safety, dangerous preparation, and high cost have not been completely resolved.

Energetic coordination polymers (ECPs) with metal atoms coordinated by highly powerful ligands to form stable networks are a new class of explosives.^{3,12–14} Metal-based coordination polymers could be potential energetic materials with inherent advantages such as reinforced structures and high heats of detonation, mechanical strength, and thermostability.^{15–18} In 2016, Shreeve proposed that ECPs can offer the opportunities for safer energetic materials (EMs).¹⁹ However, as an emerging field, enormous challenges remain in the interpretation of relationships between structure and energetic performance.^{3,20,21} Thus, rules for the rational design of EMs should be established. Most reported ECPs can function as the secondary explosives because of their low sensitivities.^{22–29} Importing an energetic heterocycle ligand to extremely sensitive transition-metal azides by coordination polymerization can be used to effectively construct π -stacked coordination polymers. These polymers serve as a new class of primary explosives with enhanced energetic performance and reduction of mechanical sensitivities.

Thus, two solvent-free ECPs, $[\text{Co}(\text{N}_3)_2(\text{atrz})]_n$ **1** and $[\text{Cd}(\text{N}_3)_2(\text{atrz})]_n$ **2** (atrz = 4,4'-azo-1,2,4-triazole), were synthesized using a simple hydrothermal method (Scheme 1).

Scheme 1. Synthetic Route of **1** and **2**



Nitrogen-rich atrz was used as a ligand because of its several advantageous properties: (i) The atrz ligand exhibits remarkable energetic properties with detonation pressure (P) of 23.50 GPa and detonation pressure (D) of 7.52 km/s as a promising secondary explosive³⁰ and enhances the energetic performance for metal azides. (ii) When the atrz ligand is incorporated into metal azides, more powerful energetic compounds such as $[\text{M}(\text{N}_3)_2(\text{atrz})]_n$ (M = divalent metal ions) can be obtained because of the six coordination nitrogen atoms of the neutral atrz ligand without hydrogen atoms. (iii) The compound atrz is a versatile ligand with six potential coordination nitrogen atoms and has been employed in constructing coordination polymers with various structures and interesting properties,^{31,32} which affords the possibility of designing atrz-based EMs.^{13,27,33} (iv) Contrary to hydrazine, the heterocycles of the atrz ligand can offer the possibility of a π -stacked structure to consolidate the system. In this study, we reported two isostructural 2D π -stacked solvent-free ECPs with high thermostabilities, high values for enthalpy of formation ($\Delta_f H^\circ$), remarkable heats of detonation, acceptable mechanical sensitivities, and low electrostatic discharge sensitivities. Compound **1** especially exhibits the highest $\Delta_f H^\circ$ among all reported primary explosives. Theoretical calculations reveal different degrees of repulsive steric clashes between the sensitive azide ions of **1** and **2**. This result can be in good agreement with the average distances of azide ions in the two compounds, leading to the different mechanical sensitivities. Furthermore, the relationships be-

tween the structures and sensitivities are discussed theoretically and experimentally.

EXPERIMENTAL SECTION

Caution! The ligand, sodium azide, reaction byproducts, and two compounds might explode under certain conditions (e.g., friction, impact, electrostatic discharge, or elevated temperatures) and generate high energy output. These compounds should not be handled by untrained individuals. These compounds should be prepared and handled with care and should be synthesized and used with small scales. Proper protective measures such as safety glass, leather gloves, a protective apron, a face shield, ear plugs, and earthed equipment should be undertaken during treatments.

Materials and Measurements. The atrz ligand was prepared according to the literature.^{30,34} All reagents purchased commercially were used without further purification. Powdered X-ray diffraction (PXRD) patterns were collected on a Rigaku Miniflex 600 diffractometer using Cu $K\alpha$ radiation ($\lambda = 0.15406$ nm) in the 2θ range of 5 – 65° . The simulated patterns were derived from the Mercury Version 1.4 software (<http://www.ccdc.cam.ac.uk/products/mercury/>). The FT-IR spectra were obtained on a PerkinElmer Spectrum using KBr disks in the range of 4000 – 400 cm^{-1} . Thermogravimetric analysis (TGA) experiments and differential scanning calorimetry (DSC) measurements were done on METTLER TOLEDO instrument in N_2 with the sample heated in an Al_2O_3 crucible at a heating rate of 5 $^\circ\text{C}\cdot\text{min}^{-1}$. Thermal decomposition residuals were analyzed with a field emission scanning electron microscope (FESEM, JSM6700F) furnished with energy dispersive X-ray spectroscopy (EDX, Oxford INCA). The combustion heats were measured by oxygen bomb calorimetry (SE-AC8018, Changsha Kaiyuan Instruments Co., LTD, China). The impact sensitivity (IS) and friction sensitivity (FS) were determined using a BAM fall hammer BFH-12 and a BAM friction apparatus FSKM-10 produced by OZM Research (Czech Republic), respectively. The electrostatic discharge sensitivities were recorded on an Xspark8 instrument manufactured by OZM Research operating with the Winspark 2 software package.

Synthesis of $[\text{Co}(\text{N}_3)_2(\text{atrz})]_n$ **1.** An aqueous solution of 3 mL of $\text{Co}(\text{NO}_3)_2\cdot 6\text{H}_2\text{O}$ (146 mg, 0.5 mmol) was added to a stirring aqueous solution (10 mL) of atrz (82 mg, 0.5 mmol) at 90 $^\circ\text{C}$ for 10 min. Then, 3 mL of NaN_3 (65 mg, 1.0 mmol) aqueous solution was added. The resultant solution was further stirred at 90 $^\circ\text{C}$ for 3 h and then filtered. Red brown crystals were obtained after 2 d. Yield: 51% (based on atrz). Calcd for $\text{C}_4\text{H}_4\text{N}_{14}\text{Co}$: C, 15.63; H, 1.30; N, 63.81%; found: C, 15.94; H, 1.39; N, 63.22%. IR (KBr pellet, cm^{-1}): 3364 s, 3113 s, 2064 vs, 1487 s, 1384 s, 1303 s, 1177 s, 1043 s, 933 w, 859 s, 697 s, 623 s, 556 s.

Synthesis of $[\text{Cd}(\text{N}_3)_2(\text{atrz})]_n$ **2.** The synthetic procedure and reactant amount for **2** were the same as those for **1** except that $\text{Co}(\text{NO}_3)_2\cdot 6\text{H}_2\text{O}$ was replaced by $\text{Cd}(\text{ClO}_4)_2\cdot 6\text{H}_2\text{O}$ (210 mg, 0.5 mmol). Yield: 56% (based on atrz). Calcd for $\text{C}_4\text{H}_4\text{N}_{14}\text{Cd}$: C, 13.31; H, 1.11; N, 54.39%; found: C, 13.50; H, 1.13; N, 53.99%. IR (KBr pellet, cm^{-1}): 3353 w, 3099 s, 2050 s, 1486 s, 1371 s, 1302 m, 1175 s, 1025 s, 968 m, 852 s, 691 s, 610 s, 541s. The two compounds were washed thoroughly with alcohol before measurement. The peak positions of the experimental PXRD patterns were consistent with the respective simulated ones, and these results indicate the pure phases of the as-synthesized **1** and **2** (Figure S1).

Crystal Structure Determination. Single crystal X-ray diffraction was carried out by Rigaku PILATUS CCD diffractometer equipped with graphite-monochromated Mo $K\alpha$ radiation ($\lambda = 0.71073$ Å) at 293 K. The intensity data sets were collected using a ω -scan technique and reduced using CrystalClear software. The structures were solved by direct methods, and the subsequent successive difference Fourier transform yielded other nonhydrogen atoms. The hydrogen atoms were calculated in idealized positions and allowed to ride on their parent atoms. The final structures were refined using a full-matrix least-squares refinement on F^2 with anisotropic thermal parameters for

all nonhydrogen atoms. All calculations were performed by the SHELXTL-2013 program.³⁵

Calculation of Intermolecular Interactions. To obtain plots of the electron density ($\rho(r)$) and reduced density gradient ($s = 1/(2(3\pi^2)^{1/3})|\nabla\rho(r)|/\rho(r)^{4/3}$), density-functional theory (DFT) calculations were performed for a selected set of **1** and **2**. Calculations were performed with the B3LYP functional³⁶ and the 6-31G* basis set using the Gaussian 09 program.³⁷ The results were analyzed by Multiwfn.³⁸

Calculation of Electronic Structures and Density of States (DOS). The calculation models were built directly from X-ray crystallographic data to calculate the energy band structures for **1** and **2**. Calculations of the electronic structures and DOS were carried out by the CASTEP code based on DFT with the GGA-PBE functional in the Materials Studio v6.0 software package.^{39,40} Energy cutoff for **1** and **2** was determined to be 700 eV, and numerical integration of Brillouin zone was employed by utilizing $3 \times 3 \times 2$ and $3 \times 2 \times 2$ Monkhorst–Pack k -point for **1** and **2**, respectively.

RESULTS AND DISCUSSION

Crystal Structure. $[Co(N_3)_2(atrz)]_n$ **1**. X-ray crystallographic analysis reveals that **1** belongs to the $P\bar{1}$ space group (Table 1).

Table 1. Crystal Data and Structure Refinement Parameters for **1** and **2**

compound	1	2
CCDC	1561308	1561310
empirical formula	C ₄ H ₄ N ₁₄ Co	C ₄ H ₄ N ₁₄ Cd
$M_r/g \text{ mol}^{-1}$	307.14	360.62
crystal system	triclinic	triclinic
space group	$P\bar{1}$	$P\bar{1}$
Z	1	1
$a/\text{\AA}$	5.2315(16)	5.3664(12)
$b/\text{\AA}$	6.0448(19)	6.2313(14)
$c/\text{\AA}$	8.497(3)	8.7401(18)
$\alpha/^\circ$	71.411(18)	70.500(18)
$\beta/^\circ$	74.31(2)	73.152(18)
$\gamma/^\circ$	79.01(2)	79.38(2)
$V/\text{\AA}^3$	243.58(14)	262.43(11)
$D_c/g \text{ cm}^{-3}$	2.094	2.282
temperature (K)	293(2)	293(2)
$F(000)$	153	174
reflms	2625	2799
GOF on F^2	1.027	1.049
$R_1 (I > 2\sigma(I))^a$	0.0432	0.0213
$wR_2 (I > 2\sigma(I))^b$	0.1071	0.0509
R_1 (all data) ^a	0.0517	0.0510
wR_2 (all data) ^b	0.1102	0.1248

$$^a R_1 = \sum(F_0 - F_c)/\sum F_0. \quad ^b wR_2 = [\sum w(F_0^2 - F_c^2)^2/\sum w(F_0^2)^2]^{1/2}.$$

The asymmetric unit of **1** consists of half a Co(II) atom, half an atrz ligand, and one azide ion (Figure S3). As illustrated in Figure 1a, each Co(II) center is six-coordinated by four nitrogen atoms from four symmetry-related azide ions and two nitrogen atoms from the two symmetry-related neutral atrz ligands to constitute a distorted octahedral geometry with the Co–N distances being in the normal range of 2.126(3)–2.181(3) Å (Table S1). Each atrz ligand displays a μ_2 - $\kappa N11$: $\kappa N11B$ coordination style to link the neighboring Co(II) atom to form an infinite 1D chain with a Co(II)⋯Co(II) distance of 11.894(8) Å. Each pair of azide ions exhibiting $\mu_{1,3}$ -bridge modes further connect two Co(II) atoms from adjacent chains with the Co(II)⋯Co(II) distance of 5.231(5) Å to produce a 2D layer (Figure 1b). These 2D layers are stacked by the face-to-face π - π interactions between interlayered triazole rings

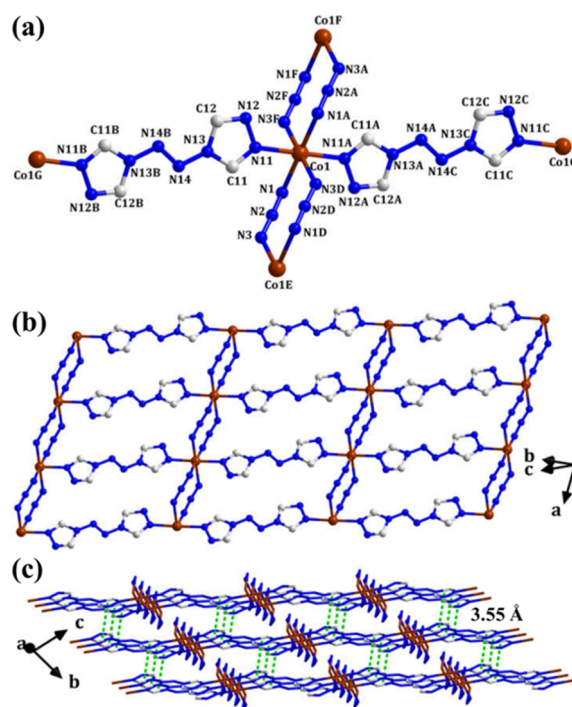


Figure 1. (a) Coordination environments of the Co(II) atom and atrz ligand of **1**. Symmetry codes: A = $2 - x, 1 - y, -z$; B = $2 - x, -y, -1 - z$; C = $x, 1 + y, 1 + z$; D = $1 - x, 1 - y, -z$; E = $-1 + x, y, z$; F = $1 + x, y, z$; G = $x, -1 + y, -1 + z$. (b) 2D layer structure of **1**. (c) The π - π stacking interaction fashion (green dotted lines) of the 2D layers for **1**. All hydrogen atoms have been omitted for clarity.

(3.55 Å) to construct the 3D supramolecular network (Figure 1c, Figure S5, and Table S2).⁴¹

$[Cd(N_3)_2(atrz)]_n$ **2**. Compound **2** is isostructural with **1** (Figure S6). Each Cd(II) atom is also six-coordinated to form the distorted octahedral coordination geometry with the Cd–N bond lengths between 2.319(3)–2.374(2) Å and the N–Cd–N angles varying from 87.67(9) to 180.0° (Table S1). Similar to **1**, the atrz ligands and azide ions in **2** bridge the Cd(II) atoms to form the 2D layers. The 2D layers are stacked *vis* the face-to-face π - π stacking interactions between interlayered triazole rings (3.51 Å) to generate the 3D supramolecular structure. Compared with metal azides, the synergistic effects of strong coordination bonds to reinforce molecular structures and π - π stacking interactions to build a closely packed 2D architecture are responsible for the relatively low mechanical sensitivities of energetic compounds **1** and **2**.

Thermal Behavior. The TGA and DSC curves of **1** and **2** are shown in Figure 2. The TGA curve of **1** reveals that a weight loss of 29.1% (calcd: 27.3%) from 208 to 249 °C is mainly due to the decomposition of N_3^- ions when the DSC curve shows a sharply exothermic peak at 246 °C (Figure 2a). Compound **1** continued to break down with continuous heating because of the decomposition of ligands. Similarly, the fast decomposition of **2** starts at 218 °C and ends at 280 °C with a weight loss of 24.4% (calcd: 23.3%) mainly ascribed to the release of N_3^- ions, which corresponds to a sharply exothermic peak at 273 °C (Figure 2b). Then, a relatively slow mass loss occurs by continuous heating with the decomposition of ligands. The thermal decomposition residuals of compounds **1** and **2** are determined using an EDX. Cobalt and carbon elements have been detected for **1**, while cadmium and carbon

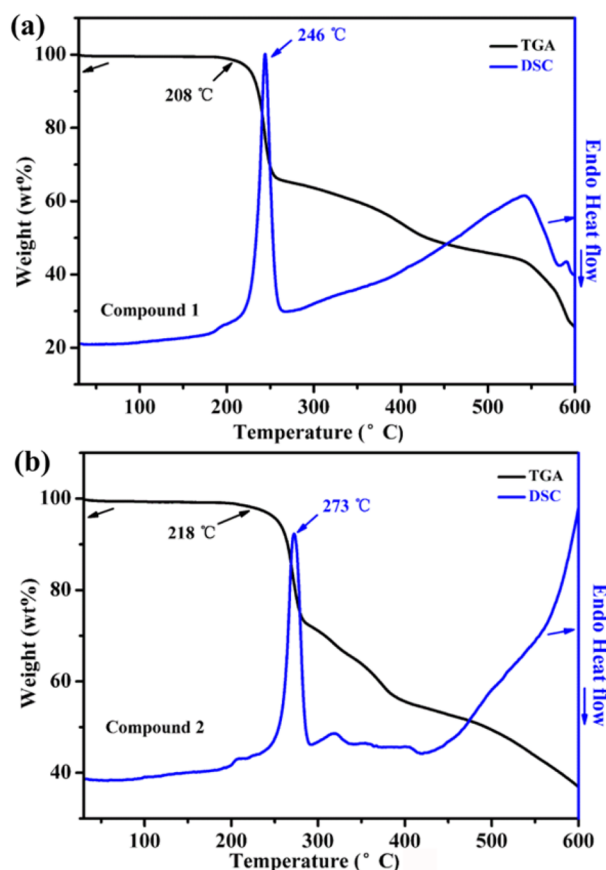
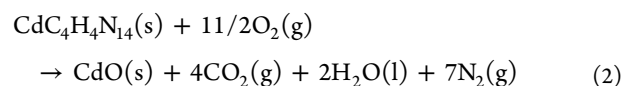
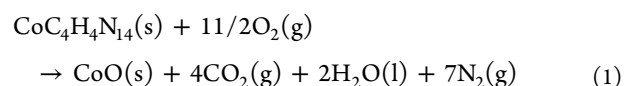


Figure 2. TGA and DSC curves of 1 (a) and 2 (b).

have been determined for 2 (Figure S7). These results suggest that the decomposition products may be similar for the two isostructural compounds. The thermal decomposition temper-

atures of 1 and 2 are higher than 200 °C to satisfy the requirements for practical applications.

Energetic Properties. Compounds 1 and 2 have high nitrogen contents with 63.81% for 1 and 54.39% for 2, which indicates 1 and 2 may serve as energetic materials. The highly positive enthalpies of formation ($\Delta_f H^\circ$) are the main energy output source of nitrogen-rich energetic compounds. To study the enthalpy of formation of 1 and 2, the constant-volume combustion heat ($\Delta_c U$) was tested by oxygen bomb calorimetry and the experimental values were 12.013 and 10.783 $\text{kJ}\cdot\text{g}^{-1}$, respectively (Supporting Information for Experimental details). The enthalpy of combustion ($\Delta_c H$) was calculated from $\Delta_c U$ with a gas volume correction: $\Delta_c H = \Delta_c U + \Delta nRT$, where Δn is the change of about the number of gas constituents in the reaction process, $R = 8.314 \text{ J}\cdot\text{mol}^{-1}\cdot\text{K}^{-1}$ and $T = 298.15 \text{ K}$. The combustion reactions are given in eqs 1 and 2 as follows:



The calculated $\Delta_c H$ values of 1 and 2 are -11.939 and $-10.745 \text{ kJ}\cdot\text{g}^{-1}$, respectively. The $\Delta_f H^\circ$ values of 1 and 2 were calculated from Hess's law as applied to eqs 3 and 4 and deduced as 4.21 and 4.08 $\text{kJ}\cdot\text{g}^{-1}$, respectively, by the known enthalpies of $\text{CoO}(\text{s}, -237.94 \text{ kJ}\cdot\text{mol}^{-1})$, $\text{CdO}(\text{s}, -258.35 \text{ kJ}\cdot\text{mol}^{-1})$, $\text{CO}_2(\text{g}, -393.51 \text{ kJ}\cdot\text{mol}^{-1})$, and $\text{H}_2\text{O}(\text{l}, -285.83 \text{ kJ}\cdot\text{mol}^{-1})$.

$$\Delta_f H^\circ[\mathbf{1}, \text{s}] = \Delta_f H^\circ[\text{CoO}, \text{s}] + 4\Delta_f H^\circ[\text{CO}_2, \text{g}] + 2\Delta_f H^\circ[\text{H}_2\text{O}, \text{l}] - \Delta_c H[\mathbf{1}, \text{s}] \quad (3)$$

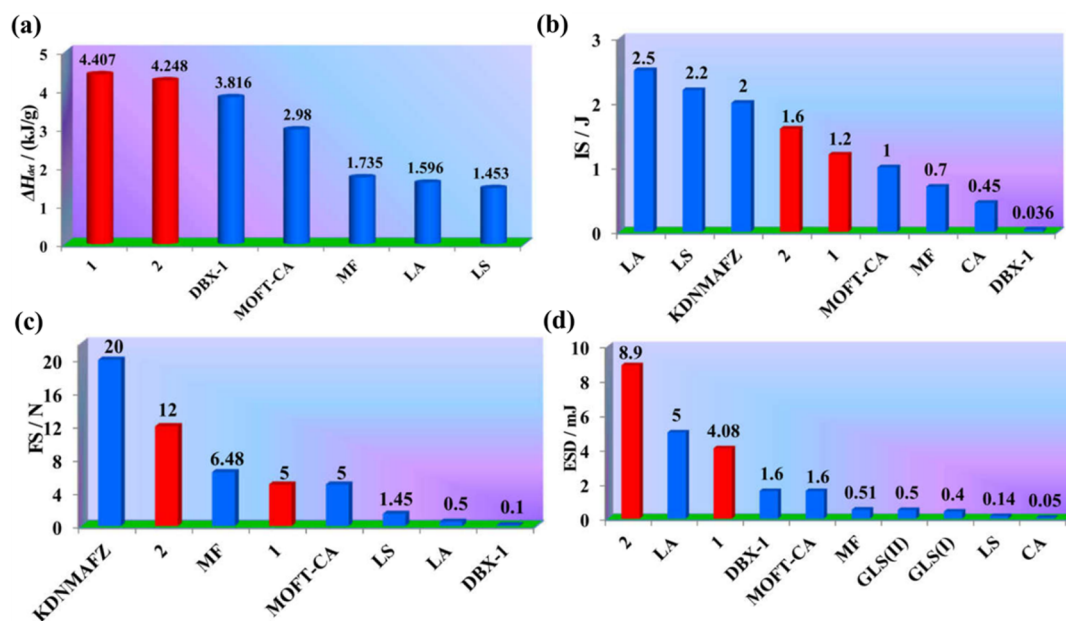


Figure 3. (a) Bar diagram representation of the ΔH_{det} values for 1, 2, MOFT-CA,⁹ DBX-1,^{45,46} and the traditional primary explosives, including MF,⁴² LA,⁶ and LS⁴² for comparison. (b) Impact sensitivities of 1, 2, LA,⁷ LS,⁷ MOFT-CA,⁹ MF,⁷ CA,⁷ KDNMAFZ,¹¹ and DBX-1.^{45,46} (c) Friction sensitivities of 1, 2, LA,⁷ LS,⁷ MOFT-CA,⁹ MF,⁷ KDNMAFZ,¹¹ and DBX-1.^{45,46} (d) Electrostatic discharge sensitivities of 1, 2, LA,⁶ LS,⁹ MOFT-CA,⁹ MF,⁷ CA,⁹ DBX-1,^{45,46} GLS(I),⁴⁹ and GLS(II).

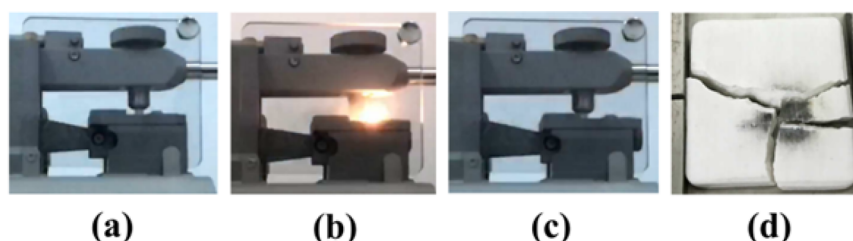
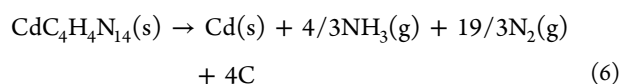
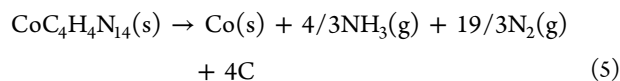


Figure 4. Explosive procedure in friction sensitivity test of **1** (about 10 mg). (a) Before friction sensitivity test; (b) friction sensitivity test of **1** at the moment of detonation; (c) after friction sensitivity test; (d) the porcelain plate being destroyed by the explosion of **1**.

$$\Delta_f H^\circ[\mathbf{2}, \text{s}] = \Delta_f H^\circ[\text{CdO}, \text{s}] + 4\Delta_f H^\circ[\text{CO}_2, \text{g}] + 2\Delta_f H^\circ[\text{H}_2\text{O}, \text{l}] - \Delta_c H[\mathbf{2}, \text{s}] \quad (4)$$

The $\Delta_f H^\circ$ values of **1** (4.21 kJ·g⁻¹) and **2** (4.08 kJ·g⁻¹) are evidently higher than those reported for KDNMAFZ (0.245 kJ·g⁻¹)¹¹ and traditional primary explosives such as LA (1.55 kJ·g⁻¹) and MF (1.35 kJ·g⁻¹).⁴² In particular, **1** possesses the highest value of $\Delta_f H^\circ$ for the hitherto known primary explosives.

EMs emit energy by detonation. Thus, ΔH_{det} is one of the most significant parameters to estimate the detonation performance. To obtain relatively accurate ΔH_{det} values, the developed Kamlet–Jacobs method adopted by Pang was selected. This method has been used to calculate ΔH_{det} of metal-based energetic materials based on the empirical Kamlet formula.⁴³ The reliability of the calculated values from the developed Kamlet–Jacobs method has been demonstrated by comparing the calculated results from the EXPLOS software.^{27,43,44} For **1** and **2**, metal, ammonia, nitrogen gas, and carbon are assumed to be explosion products (Supporting Information for the details), and the explosion reactions considered for **1** and **2** are depicted in eqs 5 and 6.



$$\Delta H_{\text{det}} = \frac{[\Delta_f H^\circ(\text{denotation products}) - \Delta_f H^\circ(\text{explosive})]}{\text{formula weight of explosive}} \quad (7)$$

The ΔH_{det} values of **1** and **2** were calculated to be 4.407 and 4.248 kJ·g⁻¹, respectively, according to eq 7 with the known $\Delta_f H^\circ$ values of Co, Cd, NH₃, N₂, and C, and the above experimentally determined $\Delta_f H^\circ$ of **1** and **2**. The ΔH_{det} values of **1** and **2** are not only two times higher than those of commercial primary explosives, such as MF (1.735 kJ·g⁻¹),⁴² LA (1.569 kJ·g⁻¹),⁶ and LS (1.453 kJ·g⁻¹),⁴² but are also higher than those of MOFT-CA (2.98 kJ·g⁻¹)⁹ and copper(I) 5-nitrotetrazolate (DBX-1) (3.816 kJ·g⁻¹)^{45,46} (Figure 3a). The high ΔH_{det} values of **1** and **2** are ascribed to the highly energetic ligand, azide ions, and many strong coordination bonds to build a closely packed 2D π -stacked architecture with powerful structural reinforcement.

To further investigate the detonation characteristics, the values of D and P of **1** and P of **2** were estimated by the developed Kamlet–Jacobs equations that have been applied to predict the

detonation performances of metal-containing explosives (see the Supporting Information).⁴³ The D and P values of **1** were calculated to be 7.672 km·s⁻¹ and 28.45 GPa, respectively, while those of **2** were 7.538 km·s⁻¹ and 28.72 GPa, respectively. The D values of **1** and **2** are comparable to that of the reported KDNMAFZ (8.138 km·s⁻¹)¹¹ and much higher than that of LA (5.920 km·s⁻¹),⁶ and the P values are comparable to those of the reported KDNMAFZ (30.1 GPa)¹¹ and the commercial primary explosive LA (33.80 GPa).⁶

Considering the safety of **1** and **2**, the impact, friction, and electrostatic discharge sensitivities (IS, FS, and ESD) were investigated by standard BAM drop hammer, standard BAM friction tester techniques, and Xspark8 apparatus operated with the Winspark 2 software package (Supporting Information for Experimental details). The collected IS, FS, and ESD data of **1**, **2**, and other primary explosives are displayed in Figure 3. The IS values of **1** and **2** are 1.2 and 1.6 J, respectively, which are comparable to those of commercial primary explosives (Figure 3b). The FS values of **1** and **2** are tested to be 5 and 12 N, respectively, both of which are less sensitive than LA with FS of 0.5 N (Figure 3c).⁷ Complete detonation with a bang to destroy the porcelain plate was observed in the FS test of **1** (about 10 mg) (Figure 4). According to the U.N. Recommendations on the Transport of Dangerous Goods, **1** belongs to extremely sensitive explosive, while **2** is considered to be a very sensitive explosive, and these compounds are acceptable for use as primary explosives.⁴⁷ The IS and FS values denote that **1** and **2** can act as potentially valuable primary explosives.

Electrostatic discharge of explosives, which is very difficult to impede, has caused several fatal accidents.⁴⁸ Thus, the electrostatic discharge sensitivity (also called electrical spark sensitivity) plays a very crucial position for EMs, especially for primary explosives. For primary explosives with poor electric conductivity (σ), electric potential produced by the accumulation of electrostatic charges can exceed the breakdown voltage of the surrounding atmosphere to bring about the occurrence of an electrostatic discharge.⁴⁹ Therefore, the σ -value of EMs is an essential factor to influence ESD.^{8,9} As, LS can easily accumulate electrostatic charges because LS is highly non-conductive with the σ -value of 5.263×10^{-15} S·m⁻¹.⁴⁹ In this study, the electric conductivities of the two compounds were tested, and the σ -values of **1** and **2** were 6.896×10^{-8} and 8.644×10^{-8} S·m⁻¹, respectively. The calculated band gaps of the two compounds (0.782 eV for **1** and 1.020 eV for **2**, Figure S10) indicate that **1** and **2** may be semiconductors.⁵⁰ The values of ESD for **1** and **2** are measured to be 4.08 and 8.90 mJ, respectively, while those of commercial LS and two modified LS, GLS (I), and GLS (II) are as low as 0.14, 0.4, and 0.5 mJ, respectively.⁴⁹ These results indicate that **1** and **2** are safer than most of the common primary explosives (Figure 3d).

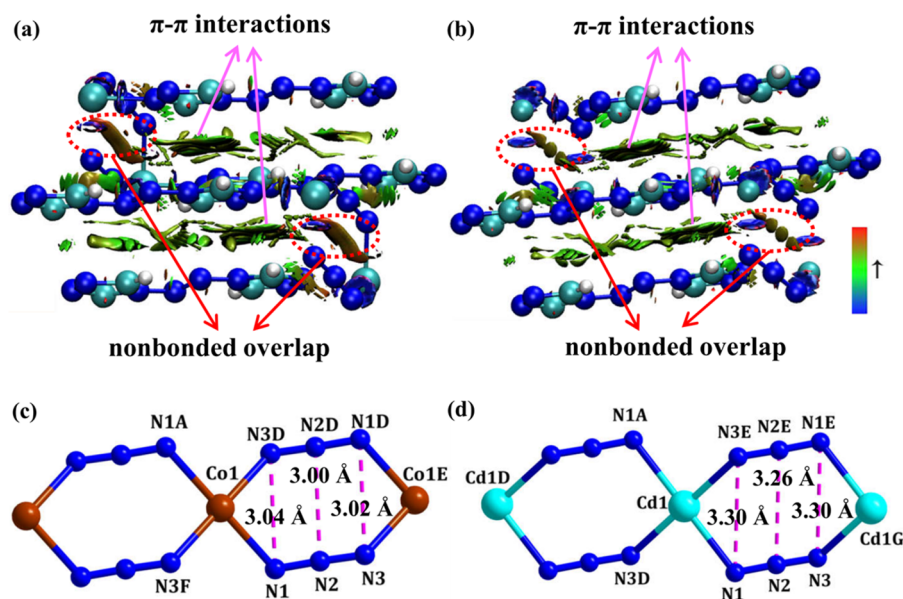


Figure 5. NIC plots of gradient isosurfaces for **1** (a) and **2** (b). The surfaces are colored on a blue-green-red (BGR) scale, ranging from -0.04 to 0.02 au. Blue indicates strong attractive interactions; green represent weak attractive interactions, and red indicates strong nonbonded overlap. The distances of nitrogen atoms (pink dotted lines) between the adjacent azide ions for **1** (c) and **2** (d).

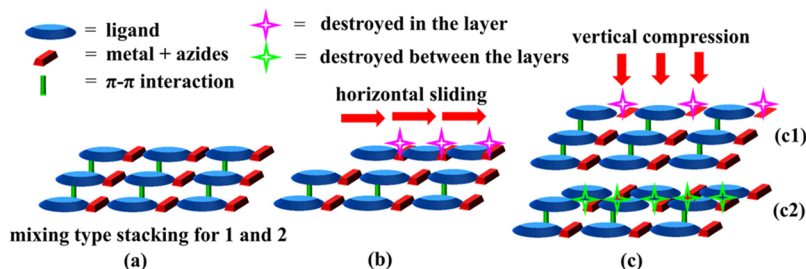


Figure 6. (a) A simplified model based on the molecular frameworks of **1** and **2**. (b) Mechanical stimulus in horizontal sliding. (c1) The azide ions in the layer destroyed by vertical compression without damaging of the π - π interactions. (c2) The π - π interactions between the layers destroyed by vertical compression.

Effects of Structure on Mechanical Sensitivities. The intramolecular interactions remarkably influence on the mechanical sensitivity of EMs. The noncovalent interactions (NCI) plots of **1** and **2** were performed by the calculation method of electron density and its reduced gradient by Yang (Figure 5).⁵¹ This calculation approach can be used to observe the differences between strong attractive interactions, van der Waals interactions, and repulsive steric clashes by analyzing the relationship between quantum-mechanical electron density (ρ) and the reduced density gradient ($s = 1/(2(3\pi^2)^{1/3})|\nabla\rho(r)|/\rho(r)^{4/3}$).⁵¹ Many studies have indicated that the face-to-face π - π interactions can effectually buffer against mechanical actions to remarkably reduce the sensitivity.^{52–54} As shown in Figure 5, the face-to-face π - π interactions between parallel rings of triazole can be clearly determined. Moreover, the corresponding NCI domains in **1** and **2** are nearly the same, which is in accordance with the distances of π - π interactions of 3.55 Å for **1** and 3.51 Å for **2**. Meanwhile, the NCI domains from the nonbonded overlap between the parallel azide ions are distinct from one another with NCI domains of **1** larger than those of **2**, which can be interpreted by the average distances of azide ions of 3.02 Å for **1** and 3.29 Å for **2** (Figures 5c and 5d). The different average distances of azide ions between the two isostructural compounds are attributed to the different atomic

radii of metal atoms as coordination centers. The stronger repulsive steric clashes between the sensitive azide ions in **1** may increase the energy of the system to facilitate the ignition of **1**.

The change in the crystal shape of EMs can be caused by the external mechanical stimuli to produce strain and absorb mechanical energy.⁵⁵ When the limit energy of EMs is exceeded by the external mechanical energy, EMs will be activated to lead to a train of explosions.⁵⁵ A simplified model has been established based on the molecular frameworks of **1** and **2** to understand the principle on how the external mechanical force triggers the explosions of the two ECPs. In Figure 6, a blue ellipsoid represents the relatively stable ligand (atrz), while the red rectangle indicates the sensitive metal azides. When the external force acts on EMs, the force can be split into two directional forces with one force resulting in the horizontal sliding and the other leading to the vertical compression. For the horizontal sliding, the force most probably activates the sensitive azides by breaking the face-to-face π - π interactions (Figure 6b). The vertical force can lead to the activation of the sensitive azides in the layer without damaging of the π - π interactions (Figure 6c1) or the destructiveness of the 2D layers with the destruction of the π - π interactions (Figure 6c2). The analytical results of NCI indicated that **1** processes

stronger repulsive steric clashes between the sensitive azide ions, and **1** should be more sensitive than **2**. In addition, the presence of unpaired electrons in the Co^{2+} ion presumably makes **1** more sensitive than **2** with the Cd^{2+} ion of the d^{10} configuration.⁵⁶ Experimental results also show that **1** with IS = 1.2 J and FS = 5 N is more sensitive than **2** with IS = 1.6 J and FS = 12 N. As primary explosives, the mechanical sensitivities of **1** and **2** can be acceptable.

CONCLUSIONS

In conclusion, the highly energetic ligand is imported into two transition-metal azides by utilizing coordination polymerization to construct two powerful and safe primary explosives. Both solvent-free ECPs exhibit high decomposition temperatures (above 200 °C), acceptable mechanical sensitivities, low electrostatic discharge sensitivities, and excellent energetic performances. Furthermore, the experimental results and theoretical analyses reveal that different repulsive steric clashes between the sensitive azide ions and various electronic configurations of the constituent metal ions are responsible for the distinct mechanical sensitivities of the two isomorphous ECPs. Notably, compound **1** possesses the highest $\Delta_f H^\circ$ (4.21 $\text{kJ}\cdot\text{g}^{-1}$) among all reported primary explosives and the ΔH_{det} values of two ECPs (4.407 $\text{kJ}\cdot\text{g}^{-1}$ for **1**, 4.248 $\text{kJ}\cdot\text{g}^{-1}$ for **2**) are both two times higher than that of the commercial LA (1.569 $\text{kJ}\cdot\text{g}^{-1}$). This study provides a new insight on the preparation of next-generation powerful and safe primary explosives. Moreover, the structure–function relationship in energetic compounds was elucidated, and the results can provide guidance for the rational design of new energetic materials.

ASSOCIATED CONTENT

Supporting Information

The Supporting Information is available free of charge on the ACS Publications website at DOI: 10.1021/acs.chemmater.7b03453.

Design strategies, experimental details, bond distances and angles, interaction distances, PXRD patterns, IR spectra, coordination environments, EDX spectra, density plots, calculated band structures, photos, and I–V plots (PDF)

Crystallographic details for $[\text{Co}(\text{N}_3)_2(\text{atrz})]_n$ (CIF)

Crystallographic details for $[\text{Cd}(\text{N}_3)_2(\text{atrz})]_n$ (CIF)

Check cif of $[\text{Co}(\text{N}_3)_2(\text{atrz})]_n$ (PDF)

Check cif of $[\text{Cd}(\text{N}_3)_2(\text{atrz})]_n$ (PDF)

AUTHOR INFORMATION

Corresponding Authors

*E-mail: zfk@fjirsm.ac.cn.

*E-mail: gcguo@fjirsm.ac.cn.

ORCID

Fa-Kun Zheng: 0000-0002-7264-170X

Guo-Cong Guo: 0000-0002-7450-9702

Notes

The authors declare no competing financial interest.

ACKNOWLEDGMENTS

This work was financially supported by National Nature Science Foundation of China (Grants 21371170 and 21601186) and the Strategic Priority Research Program of the Chinese Academy of Sciences (Grant XDB20000000).

REFERENCES

- (1) Badgular, D. M.; Talawar, M. B.; Asthana, S. N.; Mahulikar, P. P. Advances in science and technology of modern energetic materials: An overview. *J. Hazard. Mater.* **2008**, *151*, 289–305.
- (2) Talawar, M. B.; Agrawal, A. P.; Asthana, S. N. Energetic coordination compounds: synthesis, characterization and thermolysis studies on bis-(5-nitro-2H-tetrazolato-*N*²)tetraammine cobalt(III) perchlorate (BNCP) and its new transition metal (Ni/Cu/Zn) perchlorate analogues. *J. Hazard. Mater.* **2005**, *120*, 25–35.
- (3) Bushuyev, O. S.; Brown, P.; Maiti, A.; Gee, R. H.; Peterson, G. R.; Weeks, B. L.; Hope-Weeks, L. J. Ionic Polymers as a New Structural Motif for High-Energy-Density Materials. *J. Am. Chem. Soc.* **2012**, *134*, 1422–1425.
- (4) Zhai, L.; Fan, X.; Wang, B.; Bi, F.; Li, Y.; Zhu, Y. A green high-initiation-power primary explosive: synthesis, 3D structure and energetic properties of dipotassium 3,4-bis(3-dinitromethylfuran-4-oxo)furan. *RSC Adv.* **2015**, *5*, 57833–57841.
- (5) Pezous, H.; Rossi, C.; Sanchez, M.; Mathieu, F.; Dollat, X.; Charlot, S.; Conédéra, V. Fabrication, assembly and tests of a MEMS-based safe, arm and fire device. *J. Phys. Chem. Solids* **2010**, *71*, 75–79.
- (6) Fischer, D.; Klapötke, T. M.; Stierstorfer, J. Potassium 1,1'-Dinitramino-5,5'-bistetrazolate: A Primary Explosive with Fast Detonation and High Initiation Power. *Angew. Chem., Int. Ed.* **2014**, *53*, 8172–8175.
- (7) Matyáš, R.; Pachman, J. *Primary Explosives*; Springer: Heidelberg, 2013.
- (8) Pelletier, V.; Bhattacharyya, S.; Knoke, I.; Forohar, F.; Bichay, M.; Gogotsi, Y. Copper Azide Confined Inside Templated Carbon Nanotubes. *Adv. Funct. Mater.* **2010**, *20*, 3168–3174.
- (9) Wang, Q.; Feng, X.; Wang, S.; Song, N.; Chen, Y.; Tong, W.; Han, Y.; Yang, L.; Wang, B. Metal-Organic Framework Templated Synthesis of Copper Azide as the Primary Explosive with Low Electrostatic Sensitivity and Excellent Initiation Ability. *Adv. Mater.* **2016**, *28*, 5837–5843.
- (10) He, C.; Shreeve, J. M. Potassium 4,5-Bis(dinitromethyl)-furoxanate: A Green Primary Explosive with a Positive Oxygen Balance. *Angew. Chem., Int. Ed.* **2016**, *55*, 772–775.
- (11) Tang, Y.; He, C.; Mitchell, L. A.; Parrish, D. A.; Shreeve, J. M. Potassium 4,4'-Bis(dinitromethyl)-3,3'-azofurazanate: a Highly Energetic 3D Metal-Organic Framework as a Promising Primary Explosive. *Angew. Chem., Int. Ed.* **2016**, *55*, 5565–5567.
- (12) Bushuyev, O. S.; Peterson, G. R.; Brown, P.; Maiti, A.; Gee, R. H.; Weeks, B. L.; Hope-Weeks, L. J. Metal–Organic Frameworks (MOFs) as Safer, Structurally Reinforced Energetics. *Chem. - Eur. J.* **2013**, *19*, 1706–1711.
- (13) Li, S.; Wang, Y.; Qi, C.; Zhao, X.; Zhang, J.; Zhang, S.; Pang, S. 3D Energetic Metal–Organic Frameworks: Synthesis and Properties of High Energy Materials. *Angew. Chem., Int. Ed.* **2013**, *52*, 14031–14035.
- (14) Zhang, Q.; Shreeve, J. M. Metal–Organic Frameworks as High Explosives: A New Concept for Energetic Materials. *Angew. Chem., Int. Ed.* **2014**, *53*, 2540–2542.
- (15) Wang, S.-H.; Zheng, F.-K.; Wu, M.-F.; Liu, Z.-F.; Chen, J.; Guo, G.-C.; Wu, A. Q. Hydrothermal syntheses, crystal structures and physical properties of a new family of energetic coordination polymers with nitrogen-rich ligand N-[2-(1H-tetrazol-5-yl)ethyl]glycine. *CrytEngComm* **2013**, *15*, 2616–2623.
- (16) Qin, J.-S.; Zhang, J.-C.; Zhang, M.; Du, D.-Y.; Li, J.; Su, Z.-M.; Wang, Y.-Y.; Pang, S.-P.; Li, S.-H.; Lan, Y.-Q. A Highly Energetic N-Rich Zeolite-Like Metal-Organic Framework with Excellent Air Stability and Insensitivity. *Adv. Sci.* **2015**, *2*, 1500150.
- (17) Feng, Y.; Bi, Y.; Zhao, W.; Zhang, T. Anionic metal–organic frameworks lead the way to eco-friendly high-energy-density materials. *J. Mater. Chem. A* **2016**, *4*, 7596–7600.
- (18) Shang, Y.; Jin, B.; Peng, R.; Liu, Q.; Tan, B.; Guo, Z.; Zhao, J.; Zhang, Q. A novel 3D energetic MOF of high energy content: synthesis and superior explosive performance of a Pb(II) compound with 5,5'-bistetrazole-1,1'-diolate. *Dalton Trans.* **2016**, *45*, 13881–13887.

- (19) Zhang, J.; Shreeve, J. M. 3D Nitrogen-rich metal–organic frameworks: opportunities for safer energetics. *Dalton trans.* **2016**, 45, 2363–2368.
- (20) McDonald, K. A.; Seth, S.; Matzger, A. J. Coordination Polymers with High Energy Density: An Emerging Class of Explosives. *Cryst. Growth Des.* **2015**, 15, S963–S972.
- (21) Seth, S.; Matzger, A. J. Coordination Polymerization of 5,5'-Dinitro-2*H*,2*H'*-3,3'-bi-1,2,4-triazole Leads to a Dense Explosive with High Thermal Stability. *Inorg. Chem.* **2017**, 56, S61–S65.
- (22) Guo, Z.; Wu, Y.; Deng, C.; Yang, G.; Zhang, J.; Sun, Z.; Ma, H.; Gao, C.; An, Z. Structural Modulation from 1D Chain to 3D Framework: Improved Thermostability, Insensitivity, and Energies of Two Nitrogen-Rich Energetic Coordination Polymers. *Inorg. Chem.* **2016**, 55, 11064–11071.
- (23) Zhang, Y.; Zhang, S.; Sun, L.; Yang, Q.; Han, J.; Wei, Q.; Xie, G.; Chen, S.; Gao, S. A solvent-free dense energetic metal–organic framework (EMOF): to improve stability and energetic performance via *in situ* microcalorimetry. *Chem. Commun.* **2017**, 53, 3034–3037.
- (24) Shen, C.; Liu, Y.; Zhu, Z.-q.; Xu, Y.-g.; Lu, M. Self-assembly of silver(I)-based high-energy metal–organic frameworks (HE-MOFs) at ambient temperature and pressure: synthesis, structure and superior explosive performance. *Chem. Commun.* **2017**, 53, 7489–7492.
- (25) Zhang, S.; Yang, Q.; Liu, X.; Qu, X.; Wei, Q.; Xie, G.; Chen, S.; Gao, S. High-energy metal–organic frameworks (HE-MOFs): Synthesis, structure and energetic performance. *Coord. Chem. Rev.* **2016**, 307, 292–312.
- (26) Li, F.; Bi, Y.; Zhao, W.; Zhang, T.; Zhou, Z.; Yang, L. Nitrogen-Rich Salts Based on the Energetic [Monoaquabis(*N,N*-bis(1*H*-tetrazol-5-yl)amine)-zinc(II)] Anion: A Promising Design in the Development of New Energetic Materials. *Inorg. Chem.* **2015**, 54, 2050–2057.
- (27) Zhang, J.; Du, Y.; Dong, K.; Su, H.; Zhang, S.; Li, S.; Pang, S. Taming Dinitramide Anions within an Energetic Metal–Organic Framework: A New Strategy for Synthesis and Tunable Properties of High Energy Materials. *Chem. Mater.* **2016**, 28, 1472–1480.
- (28) Liu, X.; Gao, W.; Sun, P.; Su, Z.; Chen, S.; Wei, Q.; Xie, G.; Gao, S. Environmentally friendly high-energy MOFs: crystal structures, thermostability, insensitivity and remarkable detonation performances. *Green Chem.* **2015**, 17, 831–836.
- (29) Wang, S.-H.; Zheng, F.-K.; Zhang, M.-J.; Liu, Z.-F.; Chen, J.; Xiao, Y.; Wu, A.-Q.; Guo, G.-C.; Huang, J.-S. Homochiral Zinc(II) Coordination Compounds Based on In-Situ-Generated Chiral Amino Acid–Tetrazole Ligands: Circular Dichroism, Excitation Light-Induced Tunable Photoluminescence, and Energetic Performance. *Inorg. Chem.* **2013**, 52, 10096–10104.
- (30) Qi, C.; Li, S.-H.; Li, Y.-C.; Wang, Y.; Chen, X.-K.; Pang, S.-P. A novel stable high-nitrogen energetic material: 4,4'-azobis(1,2,4-triazole). *J. Mater. Chem.* **2011**, 21, 3221–3225.
- (31) Chuang, Y.-C.; Ho, W.-L.; Sheu, C.-F.; Lee, G.-H.; Wang, Y. Crystal engineering from a 1D chain to a 3D coordination polymer accompanied by a dramatic change in magnetic properties. *Chem. Commun.* **2012**, 48, 10769–10771.
- (32) Ding, B.; Wang, Y.; Liu, S.; Wu, X.; Zhu, Z.; Huo, J.; Liu, Y. A series of multi-dimensional metal–organic frameworks with *trans*-4,4'-azo-1,2,4-triazole: polymorphism, guest induced single-crystal-to-single-crystal transformation and solvatochromism. *CrystEngComm* **2015**, 17, 5396–5409.
- (33) Cohen, A.; Yang, Y.; Yan, Q.-L.; Shlomovich, A.; Petrutik, N.; Burstein, L.; Pang, S.-P.; Gozin, M. Highly Thermostable and Insensitive Energetic Hybrid Coordination Polymers Based on Graphene Oxide–Cu(II) Complex. *Chem. Mater.* **2016**, 28, 6118–6126.
- (34) Liu, X. M.; Wang, B. Y.; Xue, W.; Xie, L. H.; Zhang, W. X.; Cheng, X. N.; Chen, X. M. Magnetic variation induced by structural transformation from coordination chains to layers upon dehydration. *Dalton Trans.* **2012**, 41, 13741–13746.
- (35) Sheldrick, G. M. SHELXT-Integrated space-group and crystal-structure determination. *Acta Crystallogr., Sect. A: Found. Adv.* **2015**, 71, 3–8.
- (36) Lee, C. T.; Yang, W. T.; Parr, R. G. Development of the Colle-Salvetti correlation-energy formula into a functional of the electron density. *Phys. Rev. B: Condens. Matter Mater. Phys.* **1988**, 37, 785–789.
- (37) Frisch, M. J.; Trucks, G. W.; Schlegel, H. B.; Scuseria, G. E.; Robb, M. A.; Cheeseman, J. R.; Scalmani, G.; Barone, V.; Mennucci, B.; Petersson, G. A.; Nakatsuji, H.; Caricato, M.; Li, X.; Hratchian, H. P.; Izmaylov, A. F.; Bloino, J.; Zheng, G.; Sonnenberg, J. L.; Hada, M.; Ehara, M.; Toyota, K.; Fukuda, R.; Hasegawa, J.; Ishida, M.; Nakajima, T.; Honda, Y.; Kitao, O.; Nakai, H.; Vreven, T.; Montgomery, J. A.; Peralta, Jr., J. E.; Ogliaro, F.; Bearpark, M.; Heyd, J. J.; Brothers, E.; Kudin, K. N.; Staroverov, V. N.; Kobayashi, R.; Normand, J.; Raghavachari, K.; Rendell, A.; Burant, J. C.; Iyengar, S. S.; Tomasi, J.; Cossi, M.; Rega, N.; Millam, J. M.; Klene, M.; Knox, J. E.; Cross, J. B.; Bakken, V.; Adamo, C.; Jaramillo, J.; Gomperts, R.; Stratmann, R. E.; Yazyev, O.; Austin, A. J.; Cammi, R.; Pomelli, C.; Ochterski, J. W.; Martin, R. L.; Morokuma, K.; Zakrzewski, V. G.; Voth, G. A.; Salvador, P.; Dannenberg, J. J.; Dapprich, S.; Daniels, A. D.; Farkas, Ö.; Foresman, J. B.; Ortiz, J. V.; Cioslowski, J.; Fox, D. J. *Gaussian 09*, Revision A.02; Gaussian, Inc.: Wallingford, CT, 2009.
- (38) Lu, T.; Chen, F. Multiwfn: A Multifunctional Wavefunction Analyzer. *J. Comput. Chem.* **2012**, 33, S80–S92.
- (39) Payne, M. C.; Teter, M. P.; Allan, D. C.; Arias, T. A.; Joannopoulos, J. D. Iterative minimization techniques for *ab initio* total-energy calculations: molecular dynamics and conjugate gradients. *Rev. Mod. Phys.* **1992**, 64, 1045–1097.
- (40) Clark, S. J.; Segall, M. D.; Pickard, C. J.; Hasnip, P. J.; Probert, M. I.; Refson, K.; Payne, M. C. First principles methods using CASTEP. *Z. Kristallogr. - Cryst. Mater.* **2005**, 220, S67–S70.
- (41) Molčanov, K.; Sabljčić, I.; Kojić-Prodić, B. Face-to-face π -stacking in the multicomponent crystals of chloranilic acid, alkali hydrochloranilates, and water. *CrystEngComm* **2011**, 13, 4211–4217.
- (42) Agrawal, J. P. High Energy Materials Propellants. *Explosives and Pyrotechnics*; Wiley-VCH: Weinheim, Germany, 2010.
- (43) Wang, Y.; Zhang, J.; Su, H.; Li, S.; Zhang, S.; Pang, S. A Simple Method for the Prediction of the Detonation Performances of Metal-Containing Explosives. *J. Phys. Chem. A* **2014**, 118, 4575–4581.
- (44) Li, C.; Zhang, M.; Chen, Q.; Li, Y.; Gao, H.; Fu, W.; Zhou, Z. Three-Dimensional Metal–Organic Framework as Super Heat Resistant Explosive: Potassium 4-(5-Amino-3-Nitro-1*H*-1,2,4-Triazol-1-yl)-3,5-Dinitropyrazole. *Chem. - Eur. J.* **2017**, 23, 1490–1493.
- (45) Fronabarger, J. W.; Williams, M. D.; Sanborn, W. B.; Bragg, J. G.; Parrish, D. A.; Bichay, M. DBX-1—A Lead Free Replacement for Lead Azide. *Propellants, Explos., Pyrotech.* **2011**, 36, 541–550.
- (46) Klapötke, T. M.; Piercey, D. G.; Mehta, N.; Oyler, K. D.; Jorgensen, M.; Lenahan, S.; Salan, J. S.; Fronabarger, J. W.; Williams, M. D. Preparation of High Purity Sodium 5-Nitrotetrazolate (NaNT): An Essential Precursor to the Environmentally Acceptable Primary Explosive, DBX-1. *Z. Anorg. Allg. Chem.* **2013**, 639, 681–688.
- (47) Impact: insensitive > 40 J, less sensitive ≥ 35 J, sensitive ≥ 4 J, very sensitive ≤ 3 J; Friction: insensitive > 360 N, less sensitive = 360 N, 80 N $<$ sensitive < 360 N, very sensitive ≤ 80 N, extremely sensitive ≤ 10 N.
- (48) Skinner, D.; Olson, D.; Block-Bolten, A. Electrostatic Discharge Ignition of Energetic Materials. *Propellants, Explos., Pyrotech.* **1998**, 23, 34–42.
- (49) Li, Z.-M.; Zhou, M.-R.; Zhang, T.-L.; Zhang, J.-G.; Yang, L.; Zhou, Z.-N. The facile synthesis of graphene nanoplatelet–lead styphnate composites and their depressed electrostatic hazards. *J. Mater. Chem. A* **2013**, 1, 12710–12714.
- (50) Zheng, Z.; Jiang, X.; Zhao, J. Structural, electronic and elastic properties of several metal organic frameworks as a new kind of energetic materials. *Chem. Phys. Lett.* **2015**, 628, 76–80.
- (51) Johnson, E. R.; Keinan, S.; Mori-Sanchez, P.; Contreras-Garcia, J.; Cohen, A. J.; Yang, W. Revealing Noncovalent Interactions. *J. Am. Chem. Soc.* **2010**, 132, 6498–6506.
- (52) Zhang, C.; Wang, X.; Huang, H. π -Stacked Interactions in Explosive Crystals: Buffers against External Mechanical Stimuli. *J. Am. Chem. Soc.* **2008**, 130, 8359–8365.

(53) Zhang, J.; Zhang, Q.; Vo, T. T.; Parrish, D. A.; Shreeve, J. M. Energetic Salts with π -Stacking and Hydrogen-Bonding Interactions Lead the Way to Future Energetic Materials. *J. Am. Chem. Soc.* **2015**, *137*, 1697–1704.

(54) Zhang, J.; Mitchell, L. A.; Parrish, D. A.; Shreeve, J. M. Enforced Layer-by-Layer Stacking of Energetic Salts towards High-Performance Insensitive Energetic Materials. *J. Am. Chem. Soc.* **2015**, *137*, 10532–10535.

(55) Zhang, C. Investigation of the Slide of the Single Layer of the 1,3,5-Triamino-2,4,6-trinitrobenzene Crystal: Sliding Potential and Orientation. *J. Phys. Chem. B* **2007**, *111*, 14295–14298.

(56) Seth, S.; McDonald, K. A.; Matzger, A. J. Metal Effects on the Sensitivity of Isostructural Metal–Organic Frameworks Based on 5-Amino-3-nitro-1H-1,2,4-triazole. *Inorg. Chem.* **2017**, *56*, 10151–10154.